2
Motor-cart system: a parametric excited nonlinear system due to electromechanical coupling

The analysis of electromechanical systems is not a new subject. The interest of analyzing their dynamic behavior is reflected by the increasing amount of research in this area (see for instance [99, 84, 41, 7, 8]). In [83] there is a chapter dedicated to the coupled problem and it is remarked that it is a problem different from parametric resonance. In [37] the whole book is dedicated to the problem but the analytical treatment supposes some small parameter, a hypothesis avoided here. Recently, the problem is been intensely studied again, see [6, 1, 4], but the literature is vast.

The mutual interaction between electrical and mechanical parts leads us to analyze a very interesting nonlinear dynamical systems [64, 24, 31, 23, 10], in which the nonlinearity comes from the coupling and varies with the coupling conditions.

In this Chapter, we analyze the dynamical behavior of a simple electromechanical system composed by a cart whose motion is driven by a DC motor. The coupling between the motor and the cart is made by a mechanism called *scotch yoke* so that the motor rotational motion is transformed into a cart horizontal motion.

2.1 Dynamics of the motor-cart system

2.1.1 Electrical system: DC motor

The mathematical modeling of DC motors is based on the Kirchhoff's law [35]. It is written as

$$l\dot{c}(t) + r\ c(t) + k_e\dot{\alpha}(t) = \nu\ , \tag{2.1}$$

$$j_m\ddot{\alpha}(t) + b_m\dot{\alpha}(t) - k_e\ c(t) = -\tau(t)\ , \tag{2.2}$$

where t is the time, ν is the source voltage, c is the electric current, $\dot{\alpha}$ is the angular speed of the motor, l is the electric inductance, j_m is the inertia moment of the motor, b_m is the damping ratio in the transmission of the torque

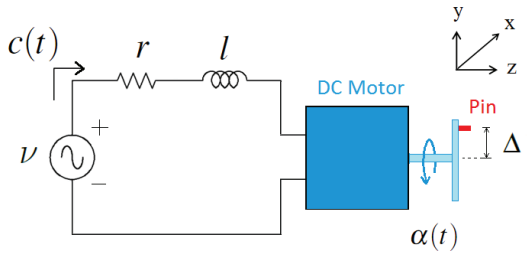

Figure 2.1: Electrical DC motor.

generated by the motor to drive the coupled mechanical system, k_e is the motor electromagnetic force constant and r is the electrical resistance. Figure 2.1 shows a sketch of the DC motor. The available torque delivered to the coupled mechanical system is represented by τ, that is the component of the torque vector $\boldsymbol{\tau}$ in the z-direction shown in Fig. 2.1. Some relevant situations when we analyze electrical motors are described as following:

- Assuming that τ and ν are constant in time, the motor achieves a steady state in which the electric current and the angular speed become constant in time. By Eqs. (2.1) and (2.2), the angular speed of the motor shaft and the current in steady state, respectively $\dot{\alpha}_{steady}$ and c_{steady}, are written as

$$\dot{\alpha}_{\text{steady}} = \frac{-\tau\, r + k_e\, \nu}{b_m\, r + k_e^2} \quad , \quad c_{\text{steady}} = \frac{\nu}{r} - \frac{k_e}{r}\left(\frac{-\tau\, r + k_e\, \nu}{b_m\, r + k_e^2}\right) . \tag{2.3}$$

- When τ is not constant in time, the angular speed of the motor shaft and the current do not reach a constant value. This kind of situation happens when, for example, a mechanical system is coupled to a motor. In this case, $\dot{\alpha}$ and c variate in time in a way that the dynamics of the motor will be influenced by the coupled mechanical system. When there is no load applied in the motor (i.e. $\tau(t) = 0$, $\forall t \in \mathbb{R}^{\geq 0}$) and the source voltage is constant in time, the motor achieves its maximum angular speed that is called the *no load speed*. It is calculated by

$$\dot{\alpha}_{\text{no load}} = \frac{k_e\, \nu}{b_m\, r + k_e^2} \quad , \quad c_{\text{no load}} = \frac{b_m}{k_e}\left(\frac{k_e\, \nu}{b_m\, r + k_e^2}\right) . \tag{2.4}$$

- The motor delivers the maximum torque, when the load applied in the motor is such that the motor does not move at all. This is called the *stall torque*. If the source voltage is constant in time, it is calculated by

$$\tau_{\text{stall}} = \frac{k_e\, \nu}{r} . \tag{2.5}$$

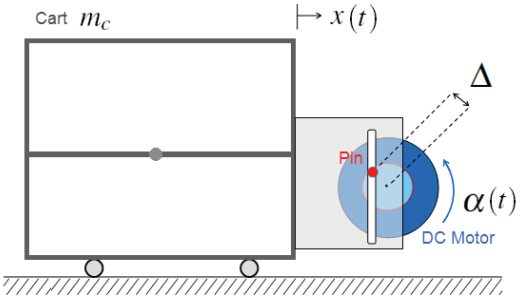

Figure 2.2: Coupled cart-motor system.

2.1.2 Cart-motor system: a master-slave relation

As described in the introduction, the system is composed by a cart whose motion is driven by the DC motor. The motor is coupled to the cart through a pin that slides into a slot machined in an acrylic plate that is attached to the cart, as shown in Fig. 2.2. The off-center pin is fixed on the disc at distance Δ of the motor shaft, so that the motor rotational motion is transformed into a cart horizontal movement. It is noticed that with this configuration, the center of mass of the mechanical system is always located in the center of mass of the cart, so its position does not change. To model the coupling between the motor and the mechanical system, the motor shaft is assumed to be rigid. Thus, the available torque vector to the coupled mechanical system, $\boldsymbol{\tau}$, can be written as

$$\boldsymbol{\tau}(t) = \boldsymbol{\Delta}(t) \times \mathbf{f}(t)\,, \tag{2.6}$$

where $\boldsymbol{\Delta} = (\Delta\ \cos\alpha(t),\ \Delta\ \sin\alpha(t),\ 0)$ is the vector related to the eccentricity of the pin, and where $\mathbf{f}$ is the coupling force between the DC motor and the cart. Assuming that there is no friction between the pin and the slot, the vector $\mathbf{f}$ only has a horizontal component, f (the horizontal force that the DC motor exerts in the cart). The available torque τ is written as

$$\tau(t) = -f(t)\ \Delta\ \sin\alpha(t)\,. \tag{2.7}$$

Due to constraints, the cart is not allowed to move in the vertical direction. The mass of the mechanical system, m, is equal the cart mass, m_c, and the horizontal cart displacement is represented by x. Since the cart is modeled as a particle, it satisfies the equation

$$m\ \ddot{x}(t) = f(t)\ . \tag{2.8}$$

Due to the system geometry, $x(t)$ and $\alpha(t)$ are related by the following constraint

$$x(t) = \Delta\ \cos\left(\alpha(t)\right). \tag{2.9}$$

Substituting Eqs. (2.7) to (2.9) into Eqs. (2.1) and (2.2), we obtain the initial value problem for the motor-cart system that is written as follows. Given a constant source voltage ν, find (α, c) such that, for all $t > 0$,

$$l\,\dot{c}(t) + r\,c(t) + k_e\,\dot{\alpha}(t) = \nu\ , \tag{2.10}$$

$$\ddot{\alpha}(t)\ \left[j_m + m\Delta^2(\sin\alpha(t))^2\right] + \dot{\alpha}\ \left[b_m + m\Delta^2\dot{\alpha}(t)\cos\alpha(t)\ \sin\alpha(t)\right] - k_e\,c(t) = 0\ , \tag{2.11}$$

with the initial conditions,

$$\dot{\alpha}(0) = 0 \quad , \quad \alpha(0) = 0 \quad , \quad c(0) = \frac{\nu}{r}\,. \tag{2.12}$$

Comparing Eq. (2.11) with Eq. (2.2), it is seen that the mechanical system influences the motor in a parametric way, [40, 65, 93, 62, 71]. The coupling torque, τ, that appears in the right side of Eq. (2.2), appears now as a time variation of the system parameters.

2.2 Dimensionless cart-motor system

In this section, the initial value problem to the motor-cart system is presented in a dimensionless form. The development of this form is a strategy to determine the dimensionless parameters of the system, which were useful in the prove of existence and asymptotic stability of a periodic orbit to this electromechanical system, discussed in Section 2.4. Beside this, the dimensionless equations were very useful for simulations, since it reduced significantly the computation time.

Consider the system of (2.10) to (2.11). Taking $\dot{\alpha}\,(t) = u\,(t)$, the system can be written as a first-order system, thus one gets that

$$\begin{aligned}
\dot{c}\,(t) &= -\frac{k_e\,u\,(t) + r\,c\,(t) - \nu}{l},\\
\dot{\alpha}\,(t) &= u\,(t)\,,\\
\dot{u}\,(t) &= \frac{-\Big(-c\,(t)\ k_t + \Delta^2\,m\,u\,(t)^2\ \cos\left(\alpha\,(t)\right)\,\sin\left(\alpha\,(t)\right) + b_m\,u\,(t)\Big)}{\Big(\Delta^2\,m\sin^2\left(\alpha\,(t)\right) + j_m\Big)}.
\end{aligned} \tag{2.13}$$

Writing

$$t = \frac{l}{r}s,\ \ \alpha\left(\frac{l\,s}{r}\right) = p\,(s)\,,\ \ u\left(\frac{l\,s}{r}\right) = \frac{r\,q\,(s)}{l},\ \ c\left(\frac{l\,s}{r}\right) = \frac{k_e\,w\,(s)}{l} \tag{2.14}$$

one gets that s is dimensionless parameter. The functions $p\,(s)$, $q\,(s)$ and $w\,(s)$ are dimensionless functions. Substituting (2.14) into (2.13) one obtains

$$\begin{aligned} w'(s) &= -w(s) - q(s) + v_0 \\ p'(s) &= q(s), \\ q'(s) &= \frac{-\Big(v_1\, q(s)^2\, \cos(p(s))\, \sin(p(s)) - v_2\, w(s) + v_3\, q(s)\Big)}{\Big(v_1 \sin^2(p(s)) + 1\Big)} \end{aligned} \tag{2.15}$$

where $'$ denotes the derivative with respect to s and v_i, $i = 0, \ldots, 3$, are dimensionless parameters given by

$$v_0 = \frac{\nu\, l}{k_e\, r}, \quad v_1 = \frac{\Delta^2\, m}{j_m}, \quad v_2 = \frac{k_e\, l\, k_t}{j_m\, r^2}, \quad v_3 = \frac{b_m\, l}{j_m\, r}. \tag{2.16}$$

The strategy to obtain the dimensionless form of the initial value problem to the motor-cart system, was writing the time t as function of the dimensionless parameter s and as function of motor parameters (the inductance, l, and resistance, r). Thus, the new dimensionless time s appeared as a parameter that is independent of the parameters of the mechanical part of the system. Due to this independence, this strategy of writing t as function of s, l, and r could be applied to the others electromechanical systems analyzed in this Thesis. We used the same dimensionless parameter s to obtain their dimensionless initial value problems.

2.3 Numerical simulations of the dynamics of the motor-cart system

Looking at Eqs. (2.10) to (2.12), it can be observed that if the nominal eccentricity of the pin, Δ, is small, the initial value problem of the motor-cart system tends to the linear system equations of the DC motor, Eq. (2.1) and (2.2), in case of no load. But as the eccentricity grows, the non-linearities become more pronounced. The nonlinearity also increases with the attached mass, m. To understand the influence of Δ and m in the dynamic behavior of the motor-cart system, a parametric excited system, simulations with different values to these system parameters were performed. The objective was to observe the graphs of the system variables, as the motor current over time, angular displacement of the motor shaft and coupling force. For computation, the initial value problem defined by Eqs. (2.10) to (2.12) has been rewritten in the dimensionless form given by Eqs. (2.15) to (2.16). Despite of using the dimensionless initial value problem for numerical simulations, the results are presented in the dimensional form because we believe that in this way they have an easier physical interpretation. The duration chosen is 2.0 s. The 4th-order Runge-Kutta method is used for the time-integration scheme with a time-

step equal to 10^{-4}. The motor parameters used in all simulations are listed in Table 2.1. The source voltage is assumed to be constant in time and equal to 2.4 V. To observe the influence of the eccentricity of the pin in the behavior

Parameter	Value
l	1.880×10^{-4} H
j_m	1.210×10^{-4} kg m^2
b_m	1.545×10^{-4} Nm/(rad/s)
r	0.307 Ω
k_e	5.330×10^{-2} V/(rad/s)

Table 2.1: Values of the motor parameters used in simulations.

of the system, the mass was fixed to 5 kg and the results of simulations with two values of Δ were compared. The selected values are $\Delta = 0.001$ m and $\Delta = 0.01$ m. For $\Delta = 0.001$ m, Figs. 2.3(a) and 2.3(b) displays $\dot{\alpha}$ as function of time and the Fast Fourier Transform (FFT) of the cart displacement, $\hat{x}$. It can be noted that the angular speed of the motor shaft oscillates with a small amplitude around 7 Hz and the FFT graph of x presents only one peak at this frequency. In contrast to this, when Δ is bigger, as $\Delta = 0.01$ m, observing Figs. 2.4(a) and 2.4(b), it is verified that the amplitude of the oscillations of $\dot{\alpha}$ grows and, due to the non-linearity effects, the FFT graph of x presents more than one peak. The first of them is at 6.56 Hz and the others are at odd multiples of this value, characterizing a periodic function.

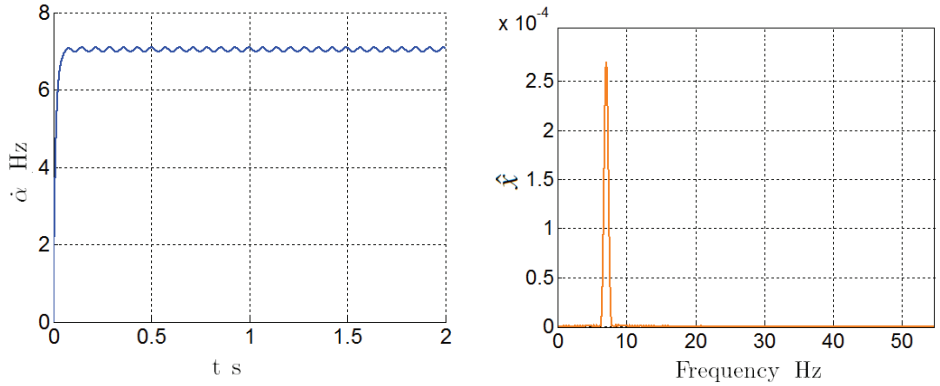

2.3(a): 2.3(b):

Figure 2.3: Motor-cart system with $\Delta = 0.001$ m: (a) angular speed of the motor shaft over time and (b) Fast Fourier Transform of the cart displacement.

As said in the introduction of this Thesis, normally problems of coupled systems are modeled as uncoupled saying that the force is imposed, and it is harmonic with frequency given by the nominal frequency of the motor. The dynamic of the motor is not considered. The graphs of Fig. 2.3(a) and 2.4(a) confirm that this hypothesis does not correspond to reality. As Δ increases,

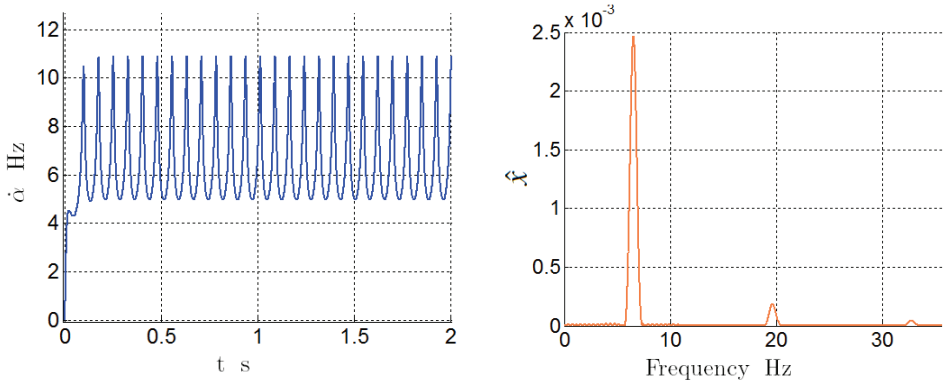

2.4(a): 2.4(b):

Figure 2.4: Motor-cart system with $\Delta = 0.01$ m: (a) angular speed of the motor shaft over time and (b) Fast Fourier Transform of the cart displacement.

increases the nonlinearity of the problem, and the hypothesis of harmonic force is inadequate since it falsifies the dynamics. Even when Δ is small, the angular speed of the motor shaft does not reach a constant value. After a transient it achieves a periodic state. It oscillates around a mean value and these oscillations are periodic. To enrich the analysis in the frequency domain, the Fast Fourier Transform of the current over time, $\hat{c}$, was computed for the two values of Δ. The results are shown in Fig. 2.5(a) and 2.5(b). It can be observed that in both cases, the FFT graph of $\hat{c}$ presents a peak at a frequency that is twice the peak frequency of the FFT $\hat{x}$ indicating the parametric excitation, [40]. In the following analysis of the motor-cart system, the nominal eccentricity

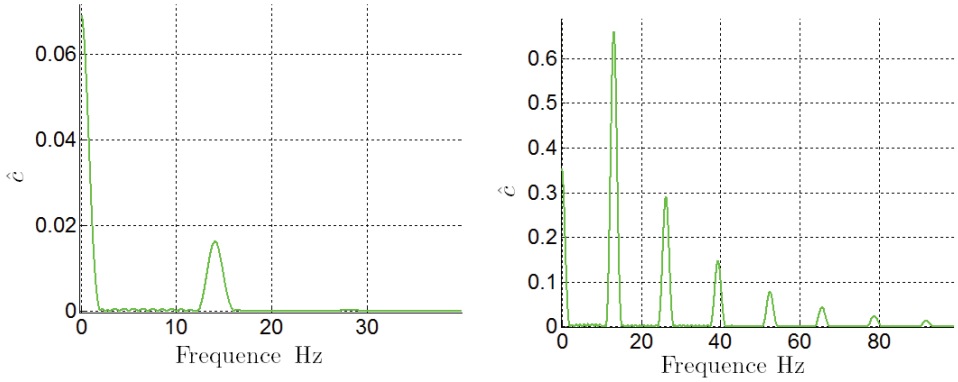

2.5(a): 2.5(b):

Figure 2.5: Motor-cart system: Fast Fourier Transform of the current (a) when $\Delta = 0.001$ m and (b) when $\Delta = 0.01$ m.

of the pin was consider to be 0.01 m. This value was selected to highlight the non-linearity effects. The results obtained to the cart displacement and current in motor over time are observed in Fig. 2.6(a) and Fig. 2.6(b). The behavior found for the current over time is similar to the behavior found for

the angular speed of the motor shaft, Fig. 2.4(a). It achieves a periodic state after a transient phase. Other graphs to be analyzed are the $f(t)$ and $\tau(t)$

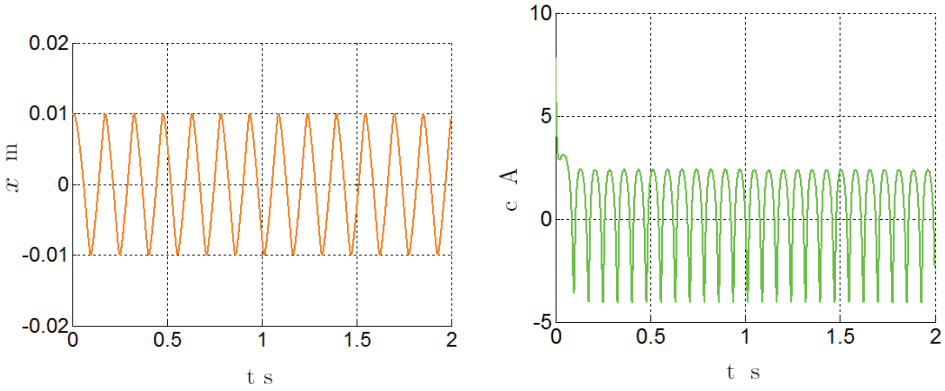

2.6(a): 2.6(b):

Figure 2.6: Motor-cart system with $\Delta = 0.01$ m: (a) cart displacement and (b) motor current over time.

variation during one cart movement cycle in the periodic state, *phase portraits* of the system, as it is shown in Figs. 2.7(a) and 2.7(b). Observing the f graph, we see that the coupling force is not harmonic. Remembering the constrain $x(t) = \Delta \cos \alpha(t)$, it is verified that the horizontal force presents its maximum value when $x(t) = -\Delta$ and its minimum value when $x(t) = \Delta$. Besides this, the coupling force changes its sign twice. Observing the τ graph, it is verified that the torque presents four points of sign change. Two of them occur when $x(t) = -\Delta$ and $x(t) = \Delta$, corresponding respectively to α multiple of π and α multiple of 2π. This changes were expected from Eq. (2.7). The others two changes occur exactly in the same cart positions that we have the sign of f changing. In each cart movement cycle, the horizontal force f and the torque τ follow once the paths shown in Fig. 2.7(a) and 2.7(b). Figures 2.8(a) and

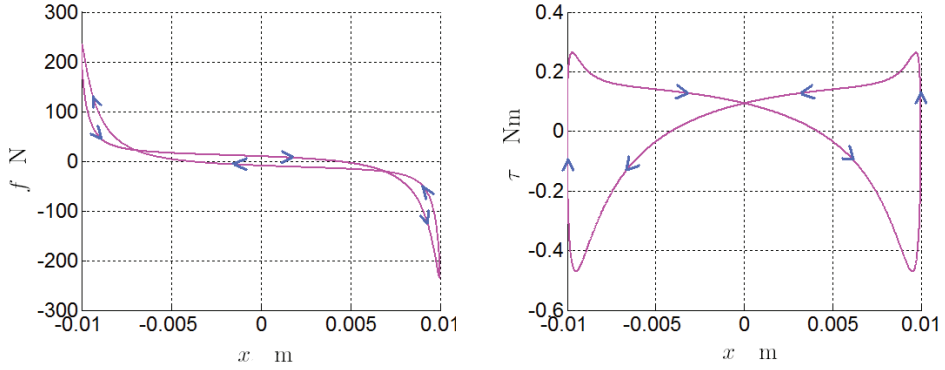

2.7(a): 2.7(b):

Figure 2.7: Motor-cart system with $\Delta = 0.01$ m: (a) horizontal force f and (b) torque τ during one cycle of the cart movement.

2.8(b) show the *phase portraits* graphs of the current variation during one cart movement cycle and the torque variation in function of the current. In the left graph, it is noted that the current presents four points of sign change in each cart movement cycle. Observing the right graph, it is verified that the current follows two times the path shown in Fig. 2.8(b). Thus, there is a relation 2:1 between the period of rotation of the disk (part of the electromechanical system) and the period of the current in the DC motor. This relation 2:1 between periods is a common phenomenon of parametric excited systems. Others phase portrait graphs are shown in Figs. 2.9(a), 2.9(b), 2.10(a) and

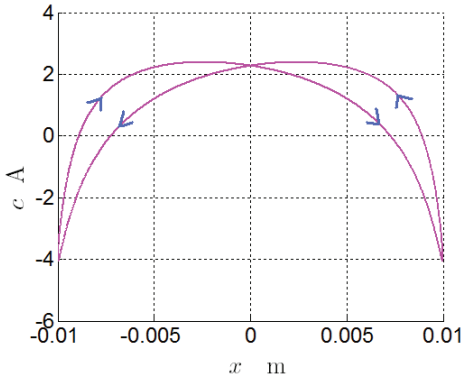

2.8(a):

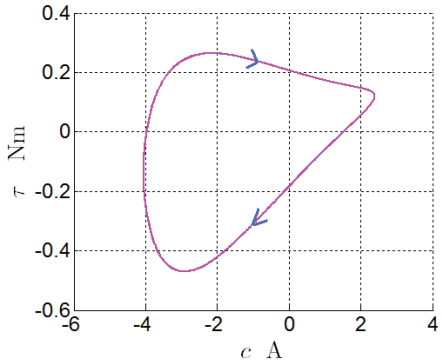

2.8(b):

Figure 2.8: Motor-cart system with $\Delta = 0.01$ m: (a) current variation during one cart movement cycle and (b) torque variation as function of the current.

2.10(b).

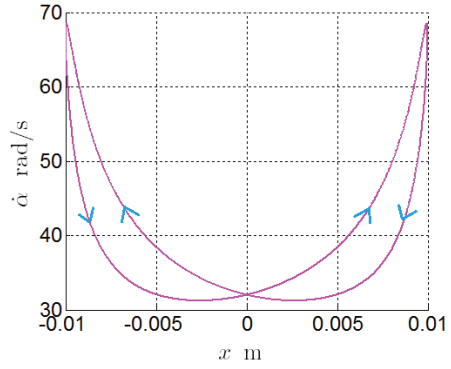

2.9(a):

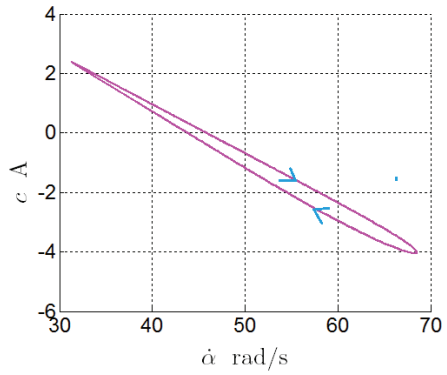

2.9(b):

Figure 2.9: Motor-cart system with $\Delta = 0.01$ m: (a) angular velocity of the motor shaft during one cart movement cycle and (b) current variation as function of the angular velocity of the motor shaft.

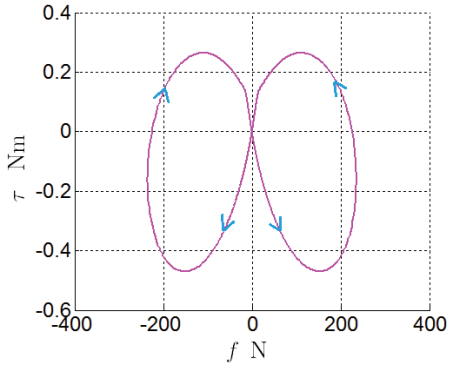

2.10(a):

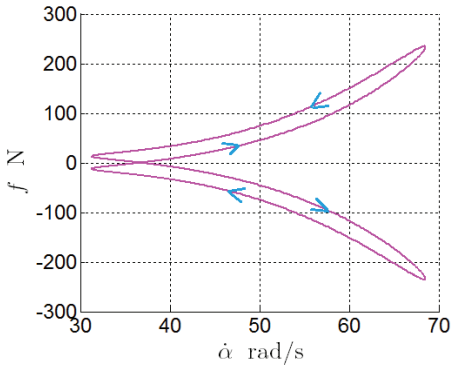

2.10(b):

Figure 2.10: Motor-cart system $\Delta = 0.01$ m: (a) torque variation as function of the horizontal force f and (b) horizontal force variation as function of the angular velocity of the motor shaft.

2.4 Asymptotically stable periodic orbit

Due to the coupling mechanism, the coupling torque, τ, variates in time. Thus, the angular speed of the motor shaft and the current are not constant values after the transient. To compare the response of the coupled systems for different values of Δ and m, the duration of one cart movement cycle, T_p, were computed in the periodic state. Figures 2.11(a) and 2.11(b) show the graphs of the computed periods as function of Δ and m. In both graphs it is observed that, the bigger Δ, or m, is, the bigger is the period of the cart movement cycle in the periodic state. It is noted too that this increment is more pronounced in relation to Δ. This result guided the development of

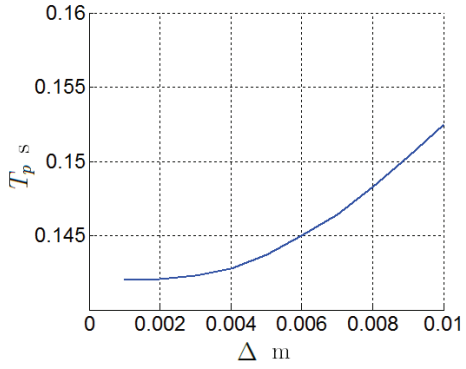

2.11(a):

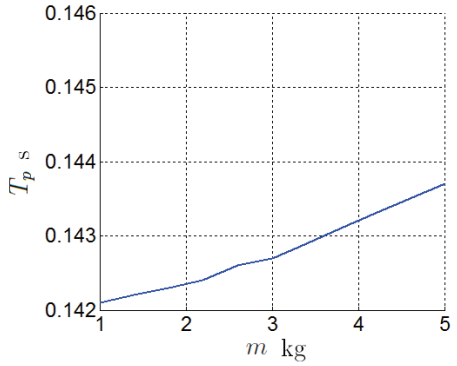

2.11(b):

Figure 2.11: Motor-cart system: period of one cart movement cycle (a) as function of Δ with $m = 5.0$ kg and (b) as function of m with $\Delta = 0.005$ m.

the paper [18], in which a similar electromechanical motor-cart system was analyzed and the existence and asymptotic stability of a periodic orbit to this system were obtained in a mathematically rigorous way. To prove the

existence and asymptotic stability of periodic orbits, the authors of [18] used the dimensionless initial value problem given by Eq. (2.15) and, assumed the following Ansatz

$$q\left(s\right) = \omega_0 + \epsilon\, z\left(s\right), \tag{2.17}$$

$$w\left(s\right) = k_1 + \epsilon\, w_1\left(s\right) \tag{2.18}$$

where

$$k_1 = \frac{v_0\, v_3}{v_3 + v_2}, \qquad \omega_0 = \frac{v_0\, v_2}{v_3 + v_2}, \tag{2.19}$$

and $v_1 = \epsilon$. Substituting the expressions of v_0, v_2 and, v_3 given in Eq. (2.16), one obtains that

$$k_1 = \frac{l\, k_e\, \nu}{r(b_m\, r + k_e^2)} = \frac{l}{r}\dot{\alpha}_{\text{no load}}, \quad \omega_0 = \frac{b_m\, \nu\, l}{k_e(b_m\, r + k_e^2)} = \frac{l}{k_e}c_{\text{no load}}. \tag{2.20}$$

From a mechanical point of view, Eq. (2.17) means that the disk, that is a part of the mechanical system modeled by Eqs. (2.10) and (2.11), will rotate at an angular speed near ω_0 (which is the velocity $\dot{\alpha}_{\text{no load}}$ in a dimensionless form) and (2.18) means that electrical current will oscillate near k_1 (which is current $c_{\text{no load}}$ in a dimensionless form).

After a mathematical proof of existence and asymptotic stability of periodic orbits, the authors of [18] obtained the following expression to the period T_p of the system

$$T_p\left(\epsilon\right) = \frac{\pi}{\omega_0} + \frac{\pi\, \omega_0\left(v_2 + \left(4\,\omega_0^2 + 1\right)\, v_3\right)\epsilon^2}{4\, E_1} + O\left(\epsilon^3\right). \tag{2.21}$$

where v_2 and v_3 are given in Eq. (2.16), and

$$E_1 = 2\,\left(v_3 + v_2\right)\, Q_1 \tag{2.22}$$

$$Q_1 = \left(4\,\omega_0^2 + 1\right)\, v_3^2 + 2\, v_2\, v_3 + v_2^2 - 8\,\omega_0^2\, v_2 + 16\,\omega_0^4 + 4\,\omega_0^2. \tag{2.23}$$

Observing this expression, one concludes that the nonlinear effects on the period are significant at second order of that expansion. Beside this, using the expressions given in Eq. (2.16), it is verified that the period grows proportionally to $m^2\,\Delta^4$, and so the growing of the period is faster in relation to Δ than to m. These results are compatible with the numerical findings shown in Figs. 2.11(a) and 2.11(b). Another interesting consequence is the following one: from Eqs. (2.17) and (2.8) it follows that the period of rotation of the disk, in the electromechanical system, is given by $\frac{2\pi}{\omega_0} + O\left(\epsilon\right)$. So, it follows from Eq. (2.21) that there is a 2:1 relation between the period of the disk and the current. Those results are compatible with the numerical findings shown previously in Figs. 2.8(b) and 2.9(b). To analyze the domain of validity

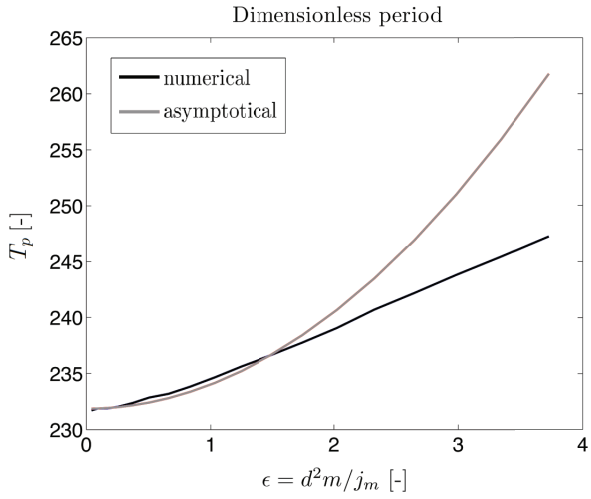

Figure 2.12: Comparison between numerical findings and the asymptotic approximation.

of the approximation of expression to the period T_p, approximations to the period were computed to different values of ϵ considering just the first and second orders terms of the Eq. (2.21). The obtained approximations were compared with the values of period obtained from numerical simulations. The results displayed in Fig. 2.12 shows that domain of validity of the approximation considering only the first and second orders terms is rather large, a fact that is not evident from perturbation theory. The paper [18] treats the problem of electromechanical coupling by a mathematical approach. As no other references dealing with this king of approach to electromechanical systems were found, we believe that [18] is a first work on the topic. Some others articles have been written in this way, as [20, 19, 17, 16]. Among the several routes for research coming from this mathematical approach, some have been studied. The objective is to prove the existence and asymptotic stability for electromechanical systems in which

- a capacitor is included in the circuit sketched in Fig. 2.1. This leads to a system with four degrees of freedom and the possibility of resonances. The guessing is that if the techniques used here can be useful for this problem.
- the cart is fixed to a wall by a linear spring and damper, as shown in Fig. 2.13. Beside this, the motor has a time-dependent voltage source given by $\nu_t(t) = \nu + \chi \sin(\omega_1 t)$. Without the spring, the system is driven by the constraint and the dynamics is a sort of master-slave relation, a very simple one. With the inclusion of the spring, the dynamics changes completely, now the constraints cannot always impose the dynamics and

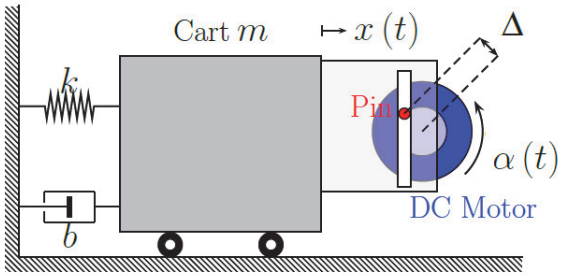

Figure 2.13: Coupled cart-motor-spring-damper system.

it is richer. The techniques used in [18] do not work any more and new techniques to show existence and stability have to be used. If the spring has a high rigidity it does not let the motor to drive the cart all the way to the end of the track and the cart oscillates around a position that depends on the rigidity of the spring and the voltage that drives the system. Some of the results already obtained for this problem are published [21].

2.5 Summary of the Chapter

The developed models revealed that the electromechanical motor-cart system is parametric excited, in which the coupling torque appears as a time variation of the system parameters. Simulations of these systems were performed for different values of Δ and m and the results of these numerical simulations, as the graphs the systems variables over time, graphs of the FFT of systems variables and *phase portraits* graphs were analyzed. From these graphs, a typical phenomenon of parametric excited systems was observed: the existence of a periodic solution with a relation 2:1 between the period of rotation of the disk and the period of the current. This result is compatible with earlier numerical findings in [42] and guided us in the development of [18], in which the existence and asymptotic stability of a periodic orbit to an electromechanical system are obtained in a mathematically rigorous way. Besides this, the nominal eccentricity of the pin of the motor, was characterized as a parameter that controls the nonlinearities of the equations of motion of the system.